NORGES TEKNISK-NATURVITENSKAPELIGE
UNIVERSITET

Preserving energy resp. dissipation in numerical PDEs, using the Average Vector Field method

by

E. Celledoni,V. Grimm, R.I. McLachlan, D.I. McLaren,
D.R.J. O'Neale, B. Owren, and G.R.W. Quispel

PREPRINT
NUMERICS NO. 7/2009

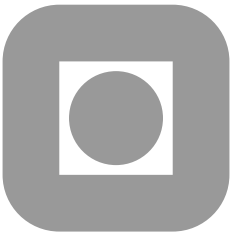

NORWEGIAN UNIVERSITY OF
SCIENCE AND TECHNOLOGY
TRONDHEIM, NORWAY

This report has URL
http://www.math.ntnu.no/preprint/numerics/2009/N7-2009.pdf
Address: Department of Mathematical Sciences, Norwegian University of Science and Technology, N-7491 Trondheim, Norway.

Preserving energy resp. dissipation in numerical PDEs, using the Average Vector Field method

E. Celledoni,V. Grimm, R.I. McLachlan, D.I. McLaren,
D.R.J. O'Neale, B. Owren, and G.R.W. Quispel

September 24, 2009

We give a systematic method for discretising Hamiltonian partial differential equations (PDEs) with constant symplectic structure, while preserving their total energy exactly. The same method, applied to PDEs with dissipative constant structure, also preserves the correct monotonic decrease of energy.

BIT Numerical Mathematics (2006)46:000-000
DOI:10.1007/s10543-000-0000-x

PRESERVING ENERGY RESP. DISSIPATION IN NUMERICAL PDEs, USING THE "AVERAGE VECTOR FIELD" METHOD *

E. CELLEDONI[1], V. GRIMM[2], R.I. MCLACHLAN[3], D.I. MCLAREN[4], D.R.J. O'NEALE[5], B. OWREN[6], G.R.W. QUISPEL[7]

[1] *Department of Mathematical Sciences, NTNU 7491 Trondheim, Norway. email: elenac@math.ntnu.no*

[2] *Department of Mathematics, Friedrich-Alexander-Universität Erlangen-Nürnberg, Martensstr. 3, D–91058 Erlangen, Germany. email: grimm@am.uni-erlangen.de*

[3] *Institute of Fundamental Sciences, Massey University, Private Bag 11-222 Palmerston North, New Zealand 5301. email: r.mclachlan@massey.ac.nz*

[4] *Department of Mathematics and Statistics, La Trobe University, Victoria 3086, Australia. email: D.McLaren@latrobe.edu.au*

[5] *Department of Mathematics and Statistics, La Trobe University, Victoria 3086, Australia. email: D.O'Neale@latrobe.edu.au*

[6] *Department of Mathematical Sciences, NTNU 7491 Trondheim, Norway. email: Brynjulf.Owren@math.ntnu.no*

[7] *Department of Mathematics and Statistics, La Trobe University, Victoria 3086, Australia. email: R.Quispel@latrobe.edu.au*

Abstract.

We give a systematic method for discretising Hamiltonian partial differential equations (PDEs) with constant symplectic structure, while preserving their energy exactly. The same method, applied to PDEs with constant dissipative structure, also preserves the correct monotonic decrease of energy. The method is illustrated by many examples. In the Hamiltonian case these include: the sine-Gordon, Korteweg-de Vries, nonlinear Schrödinger, (linear) time-dependent Schrödinger, and Maxwell equations. In the dissipative case the examples are: the Allen-Cahn, Cahn-Hilliard, Ginzburg-Landau, and Heat equations.

AMS subject classification (2000): 65L12, 65M06, 65N22, 65P10

Key words: Average vector field method, Hamiltonian PDEs, dissipative PDEs, time integration

1 Introduction

"The opening line of *Anna Karenina*, 'All happy families resemble one another, but each unhappy family is unhappy in its own way', is a useful metaphor for the relationship between computational ordinary differential equations (ODEs) and computational partial differential equations (PDEs). ODEs are a happy family – perhaps they do not resemble each other, but, at the very least, we can treat

*Received **. Revised **. Communicated by **.

them by a relatively small compendium of computational techniques... PDEs are a huge and motley collection of problems, each unhappy in its own way" (Quote from A. Iserles' book [8]).

Whereas there is much truth in the above quote, in this paper we set out to convince the reader that, as far as conservation or dissipation of energy is concerned, many PDEs form part of one big happy family (cf. also [9]) that, after a very straightforward and uniform semi-discretisation, may actually be solved by a single unique geometric integration method – the so-called average vector field method – while preserving the correct conservation, respectively, dissipation of energy. The concept of 'energy' has far-reaching importance throughout the physical sciences [4]. Therefore a single procedure, as presented here, that correctly conserves, resp. dissipates, energy for linear as well as nonlinear, low-order as well as high-order, PDEs would seem to be worth while.

We consider evolutionary PDEs with independent variables $(x,t) \in \mathbb{R}^d \times \mathbb{R}$, functions u belonging to a Banach space $\mathcal{B}$ with values[1] $u(x,t) \in \mathbb{R}^m$, and PDEs of the form

$$\dot{u} = \mathcal{D}\frac{\delta \mathcal{H}}{\delta u}, \tag{1.1}$$

where $\mathcal{D}$ is a constant linear differential operator, the dot denotes $\frac{\partial}{\partial t}$, and

$$\mathcal{H}[u] = \int_\Omega H(x; u^{(n)})\, dx \tag{1.2}$$

where Ω is a subset of $\mathbb{R}^d \times \mathbb{R}$, and $dx = dx_1 dx_2 \dots dx_d$. $\frac{\delta \mathcal{H}}{\delta u}$ is the variational derivative of $\mathcal{H}$ in the sense that

$$\frac{d}{d\epsilon}\mathcal{H}[u + \epsilon v]\big|_{\epsilon=0} = \int_\Omega \frac{\delta \mathcal{H}}{\delta u} v\, dx, \tag{1.3}$$

for all $u, v \in \mathcal{B}$ (cf. [16]). For example, if $d = m = 1$,

$$\mathcal{H}[u] = \int_\Omega H(x; u, u_x, u_{xx}, \dots)\, dx, \tag{1.4}$$

then

$$\frac{\delta \mathcal{H}}{\delta u} = \frac{\partial H}{\partial u} - \partial_x \left(\frac{\partial H}{\partial u_x}\right) + \partial_x^2 \left(\frac{\partial H}{\partial u_{xx}}\right) - \cdots, \tag{1.5}$$

when the boundary terms are zero.

Similarly, for general d and m, we obtain

$$\frac{\delta \mathcal{H}}{\delta u_l} = \frac{\partial H}{\partial u_l} - \sum_{k=1}^{d} \frac{\partial}{\partial x_k}\left(\frac{\partial H}{\partial u_{l,k}}\right) + \dots, \quad l = 1, \dots, m. \tag{1.6}$$

[1] Although it is generally real-valued, the function u may also be complex-valued, for example, the nonlinear Schrödinger equation.

We consider Hamiltonian systems of the form (1.1), where $\mathcal{D}$ is a constant skew symmetric operator (cf. [16]) and $\mathcal{H}$ the energy (Hamiltonian). In this case, we prefer to designate the differential operator in (1.1) with $\mathcal{S}$ instead of $\mathcal{D}$. The PDE preserves the energy because $\mathcal{S}$ is skew-adjoint with respect to the L_2 inner product, i.e.

$$\int_\Omega u\mathcal{S}u\,dx = 0, \quad \forall u \in \mathcal{B}. \tag{1.7}$$

The system (1.1) has $\mathcal{I} : \mathcal{B} \to \mathbb{R}$ as an integral if $\dot{\mathcal{I}} = \int_\Omega \frac{\delta \mathcal{I}}{\delta u}\mathcal{S}\frac{\delta \mathcal{H}}{\delta u}\,dx = 0$. Integrals $\mathcal{C}$ with $\mathcal{D}\frac{\delta \mathcal{C}}{\delta u} = 0$ are called Casimirs.

Besides PDEs of type (1.1) where $\mathcal{D}$ is skew-adjoint, we also consider PDEs of type (1.1) where $\mathcal{D}$ is a constant negative (semi)definite operator with respect to the L_2 inner product, i.e.

$$\int_\Omega u\mathcal{D}u\,dx \leq 0, \quad \forall u \in \mathcal{B}. \tag{1.8}$$

In this case, we prefer to designate the differential operator $\mathcal{D}$ with $\mathcal{N}$ and the function $\mathcal{H}$ is a Lyapunov function, since then the system (1.1), i.e.

$$\dot{u} = \mathcal{N}\frac{\delta \mathcal{H}}{\delta u}, \tag{1.9}$$

has $\mathcal{H}$ as a Lyapunov function, i.e. $\dot{\mathcal{H}} = \int_\Omega \frac{\delta \mathcal{H}}{\delta u}\mathcal{N}\frac{\delta \mathcal{H}}{\delta u}\,dx \leq 0$. We will refer to systems (1.1) with a skew-adjoint $\mathcal{S}$ and an energy $\mathcal{H}$ as conservative and to systems (1.1) with a negative (semi)definite operator $\mathcal{N}$ and a Lyapunov function $\mathcal{H}$ as dissipative.

Conservative PDEs (1.1) can be semi-discretised in "skew-gradient" form

$$\dot{u} = \overline{\mathcal{S}}\nabla\overline{\mathcal{H}}(u), \qquad \overline{\mathcal{S}}^T = -\overline{\mathcal{S}}, \tag{1.10}$$

when $\mathcal{D} = \mathcal{S}$ is skew-adjoint. $u \in \mathbb{R}^k$, and here, and in the following, we will always denote the discretisations with bars. $\overline{\mathcal{H}}$ is chosen in such a way that $\overline{\mathcal{H}}\Delta x$ is an approximation to $\mathcal{H}$.

LEMMA 1.1. *Let*

$$\mathcal{H}[u] = \int_\Omega H(x; u^{(n)})dx, \tag{1.11}$$

and let $\overline{\mathcal{H}}\Delta x$ be any consistent (finite difference) approximation to $\mathcal{H}$ (where $\Delta x := \Delta x_1 \Delta x_2 \dots \Delta x_d$). Then the discrete analogue of the variational derivative $\dfrac{\delta \mathcal{H}}{\delta u}$ is given by $\nabla\overline{\mathcal{H}}$. The proof is given in the appendix.

It is worth noting that the above lemma also applies directly when the approximation to $\mathcal{H}$ is obtained by a spectral discretization, since such an approximation can be viewed as a finite difference approximation where the finite difference

stencil has the same number of entries as the number of grid points on which it is defined.

The operator ∇ is the standard gradient, which replaces the variational derivative because we are now working in a finite (although large) number of dimensions (cf. e.g. (1.6)).

When dealing with (semi-)discrete systems we use the notation $u_{j,n}$ where the index j corresponds to increments in space and n to increments in time. That is, the point $u_{j,n}$ is the discrete equivalent of $u(a + j\Delta x, t_0 + n\Delta t)$ where $x \in [a, b]$ and where t_0 is the initial time. In most of the equations we present, one of the indices is held constant, in which case, for simplicity, we drop it from the notation. For example, we use u_j to refer to the values of u at different points in space and at a fixed time level.

THEOREM 1.2. *Let $\overline{\mathcal{S}}$ (resp. $\overline{\mathcal{N}}$) be any consistent constant skew (resp. negative-definite) matrix approximation to $\mathcal{S}$ (resp. $\mathcal{N}$). Let $\overline{\mathcal{H}}\Delta x$ be any consistent (finite difference) approximation to $\mathcal{H}$. Finally, let*

$$f(u) := \overline{\mathcal{S}}\nabla\overline{\mathcal{H}}(u) \qquad (\textit{resp. } f(u) := \overline{\mathcal{N}}\nabla\overline{\mathcal{H}}(u)), \tag{1.12}$$

and let u_n be the solution of the average vector field (AVF) method

$$\frac{u_{n+1} - u_n}{\Delta t} = \int_0^1 f((1-\xi)u_n + \xi u_{n+1})\, d\xi, \tag{1.13}$$

applied to equation (1.12). Then the semidiscrete energy $\overline{\mathcal{H}}$ is preserved exactly (resp. dissipated monotonically):

$$\overline{\mathcal{H}}(u_{n+1}) = \overline{\mathcal{H}}(u_n) \qquad (\textit{resp } \overline{\mathcal{H}}(u_{n+1}) \leq \overline{\mathcal{H}}(u_n)).$$

$\overline{\mathcal{H}}$ is preserved since

$$\dot{\overline{\mathcal{H}}} = \left(\nabla\overline{\mathcal{H}}\right)^T \overline{\mathcal{S}}\nabla\overline{\mathcal{H}} = 0. \tag{1.14}$$

Discretisations of this type can be given for pseudospectral, finite-element, Galerkin and finite-difference methods (cf. [12, 13]); for simplicity's sake, we will concentrate on finite-difference methods, though we include one example of a pseudospectral method for good measure.

The AVF method was recently [17] shown to preserve the energy $\overline{\mathcal{H}}$ exactly for any vector field f of the form $f(u) = \overline{\mathcal{S}}\nabla\overline{\mathcal{H}}(u)$, where $\overline{\mathcal{H}}$ is an arbitrary function, and $\overline{\mathcal{S}}$ is any **constant** skew matrix [2]. The AVF method is related to discrete gradient methods (cf. [11]).

If $\mathcal{D}$ is a constant negative-definite operator, then the dissipative PDE (1.1) can be discretized in the form

$$\dot{u} = \overline{\mathcal{N}}\nabla\overline{\mathcal{H}}(u), \tag{1.15}$$

[2]The relationship of (1.13) to Runge-Kutta methods was explored in [3].

where $\overline{\mathcal{N}}$ is a negative (semi)definite matrix and $\overline{\mathcal{H}}$ is a discretisation as above.

That is, $\overline{\mathcal{H}}$ is a Lyapunov-function for the semi-discretized system, since

$$\dot{\overline{\mathcal{H}}} = \left(\nabla\overline{\mathcal{H}}\right)^T \overline{\mathcal{N}}\nabla\overline{\mathcal{H}} \leq 0. \tag{1.16}$$

The AVF method (1.13) again preserves this structure, i.e. we have

$$\overline{\mathcal{H}}(u_{n+1}) \leq \overline{\mathcal{H}}(u_n), \tag{1.17}$$

and $\overline{\mathcal{H}}$ is a Lyapunov function for the discrete system. Taking the scalar product of (1.13) with $\int_0^1 \nabla\overline{\mathcal{H}}((1-\xi)u_n + \xi u_{n+1})\,d\xi$ on both sides of the equation yields

$$\frac{1}{\Delta t}\int_0^1 (u_{n+1}-u_n)\cdot\nabla\overline{\mathcal{H}}((1-\xi)u_n + \xi u_{n+1})\,d\xi \leq 0, \tag{1.18}$$

i.e.

$$\frac{1}{\Delta t}\int_0^1 \frac{d}{d\xi}\overline{\mathcal{H}}((1-\xi)u_n + \xi u_{n+1})\,d\xi \leq 0, \tag{1.19}$$

and therefore

$$\frac{1}{\Delta t}(\overline{\mathcal{H}}(u_{n+1}) - \overline{\mathcal{H}}(u_n)) \leq 0. \tag{1.20}$$

Our purpose is to show that the procedure described above, namely

1. Discretize the energy functional $\mathcal{H}$ using any (consistent) approximation $\overline{\mathcal{H}}\Delta x$
2. Discretize $\mathcal{D}$ by a constant skew-symmetric (resp. negative (semi)definite) matrix
3. Apply the AVF method

can be generally applied and leads, in a systematic way, to energy-preserving methods for conservative PDEs and energy-dissipating methods for dissipative PDEs. We shall demonstrate the procedure by going through several well-known nonlinear and linear PDEs step by step. In particular we give examples of how to discretise nonlinear conservative PDEs (in subsection 2.1), linear conservative PDEs (in subsection 2.2), nonlinear dissipative PDEs (in subsection 3.1), and linear dissipative PDEs (in subsection 3.2).

2 Conservative PDEs

2.1 Nonlinear conservative PDEs

EXAMPLE 2.1. *Sine-Gordon equation:*
Continuous:

$$\frac{\partial^2\varphi}{\partial t^2} = \frac{\partial^2\varphi}{\partial x^2} - \alpha\sin\varphi. \tag{2.1}$$

The Sine-Gordon equation is of type (1.1) with

$$\mathcal{H} = \int \left[\frac{1}{2}\pi^2 + \frac{1}{2}\left(\frac{\partial \varphi}{\partial x}\right)^2 + \alpha\,(1-\cos\varphi) \right] dx, \tag{2.2}$$

where $u := \begin{pmatrix} \varphi \\ \pi \end{pmatrix}$ and

$$\mathcal{S} = \begin{pmatrix} 0 & 1 \\ -1 & 0 \end{pmatrix}. \tag{2.3}$$

(Note that it follows that $\pi = \frac{\partial \varphi}{\partial t}$.)

Boundary conditions: periodic, $u(-20,t) = u(20,t)$.

Semi-discrete: finite differences[3]

$$\overline{\mathcal{H}}_{fd} = \sum_j \left[\frac{1}{2}\pi_j^2 + \frac{1}{2(\Delta x)^2}(\varphi_{j+1}-\varphi_j)^2 + \alpha\,(1-\cos\varphi_j) \right]. \tag{2.4}$$

$$\overline{\mathcal{S}} = \begin{pmatrix} 0 & \mathrm{id} \\ -\mathrm{id} & 0 \end{pmatrix}. \tag{2.5}$$

The resulting system of ordinary differential equations is

$$\begin{bmatrix} \dot{\boldsymbol{\varphi}} \\ \dot{\boldsymbol{\pi}} \end{bmatrix} = \overline{\mathcal{S}}\nabla\overline{\mathcal{H}}_{fd} = \begin{bmatrix} \boldsymbol{\pi} \\ \frac{1}{\Delta x^2} L\boldsymbol{\varphi} - \alpha \sin \boldsymbol{\varphi} \end{bmatrix}, \tag{2.6}$$

where L is the circulant matrix

$$L = \begin{bmatrix} -2 & 1 & & 1 \\ 1 & \ddots & \ddots & \\ & \ddots & \ddots & 1 \\ 1 & & 1 & -2 \end{bmatrix}.$$

We have used the bold variables $\boldsymbol{\varphi}$ and $\boldsymbol{\pi}$ for the finite dimensional vectors $[\varphi_1, \varphi_2, \ldots, \varphi_N]^\top$, *et cetera*, which replace the functions π and φ in the (semi-) discrete case. Where necessary, we will write $\boldsymbol{\varphi}_n$, *et cetera* to denote the vector $\boldsymbol{\varphi}$ at time $t_0 + n\Delta t$.

The integral in the AVF method can be calculated exactly to give[4]

$$\frac{1}{\Delta t}\begin{bmatrix} \boldsymbol{\varphi}_{n+1} - \boldsymbol{\varphi}_n \\ \boldsymbol{\pi}_{n+1} - \boldsymbol{\pi}_n \end{bmatrix} = \begin{bmatrix} (\boldsymbol{\pi}_{n+1} + \boldsymbol{\pi}_n)/2 \\ L(\boldsymbol{\varphi}_{n+1} + \boldsymbol{\varphi}_n)/2 - \alpha(\cos\boldsymbol{\varphi}_{n+1} - \cos\boldsymbol{\varphi}_n)/(\boldsymbol{\varphi}_{n+1} - \boldsymbol{\varphi}_n) \end{bmatrix}. \tag{2.7}$$

[3]Summations of the form $\sum_j$ mean $\sum_{j=0}^{N-1}$ unless stated otherwise.

[4]For numerical computations, care must be taken to avoid problems when the difference $\boldsymbol{\varphi}_{n+1} - \boldsymbol{\varphi}_n$ in the denominator of (2.7) becomes small. We used the sum-to-product identity $\cos a - \cos b = -2\sin((a+b)/2)\sin((a-b)/2)$ to give a more numerically amenable expression.

Semi-discrete: spectral discretization

Instead of using finite differences for the discretization of the spatial derivative in (2.2), one may use a spectral discretization. This can be thought of as replacing φ with its Fourier series, truncated after N terms, where N is the number of spatial intervals, and differentiating the Fourier series. This can be calculated, using the discrete Fourier transform[5] (DFT), as $\mathcal{F}_N^{-1} d_N \mathcal{F}_N \boldsymbol{\varphi}$ where $\mathcal{F}_N$ is the matrix of DFT coefficients with entries given by $[\mathcal{F}_N]_{n,k} = \omega_N^{nk}$, $\omega_N = e^{-i2\pi/N}$ Additionally, $[\mathcal{F}_N^{-1}]_{n,k} = \frac{1}{N}\omega_N^{-nk}$ and d_N is a diagonal matrix whose (non-zero) entries are the scaled wave-numbers[6] $[d_N]_{k,k} = i2\pi k/l$, $k = \frac{-N}{2}+1, \ldots, \frac{N}{2}$, (for N even), where $l = b-a$ is the extent of the spatial domain; that is $l/N = \Delta x$. (For more details on properties of the DFT and its application to spectral methods see [2] and [18].)

$$\overline{\mathcal{H}}_{sp} = \sum_j \left[\frac{1}{2}\pi_j^2 + \frac{1}{2}\left[\mathcal{F}_N^{-1} d_N \mathcal{F}_N \boldsymbol{\varphi}\right]_j^2 + \alpha(1-\cos\varphi_j) \right], \tag{2.8}$$

$$\overline{\mathcal{S}} = \begin{pmatrix} 0 & \mathrm{id} \\ -\mathrm{id} & 0 \end{pmatrix}. \tag{2.9}$$

The resulting system of ODEs is then given by

$$\begin{bmatrix} \dot{\boldsymbol{\varphi}} \\ \dot{\boldsymbol{\pi}} \end{bmatrix} = \overline{\mathcal{S}} \nabla \overline{\mathcal{H}}_{sp} = \begin{bmatrix} \boldsymbol{\pi} \\ -(\mathcal{F}_N^{-1} D_N \mathcal{F}_N)^\top (\mathcal{F}_N^{-1} d_N \mathcal{F}_N \boldsymbol{\varphi}) - \alpha \sin \boldsymbol{\varphi} \end{bmatrix}, \tag{2.10}$$

where $[D_N]_{n,k} = \theta_k$. Again, the integral in the AVF method can be calculated exactly to give

$$\frac{\boldsymbol{\varphi}_{n+1} - \boldsymbol{\varphi}_n}{\Delta t} = (\boldsymbol{\pi}_{n+1} + \boldsymbol{\pi}_n)/2, \tag{2.11}$$

$$\frac{\boldsymbol{\pi}_{n+1} - \boldsymbol{\pi}_n}{\Delta t} = -(\mathcal{F}_N^{-1} D_N \mathcal{F}_N)^\top (\mathcal{F}_N^{-1} d_N \mathcal{F}_N)(\boldsymbol{\varphi}_{n+1} + \boldsymbol{\varphi}_n)/2 - \alpha(\cos\boldsymbol{\varphi}_{n+1} - \cos\boldsymbol{\varphi}_n)/(\boldsymbol{\varphi}_{n+1} - \boldsymbol{\varphi}_n). \tag{2.12}$$

Initial conditions and numerical data for both discretizations:

Spatial domain, number N of spatial intervals, and time-step size Δt used were [7]

$$x \in [-20, 20], \qquad N = 200, \qquad \Delta t = 0.01, \qquad \text{parameter: } \alpha = 1.$$

[5] In practice, one uses the fast Fourier transform algorithm to calculate the DFTs in $\mathcal{O}(N \log N)$ operations.

[6] Care must be taken with the ordering of the wave numbers since different computer packages use different effective orderings of the DFT/IDFT matrices in their algorithms. Additionally, one must ensure that all modes of the Fourier spectrum are treated symmetrically — for N even, this requires replacing the $k = \frac{N}{2}$ entry with zero. For the FFT/IFFT algorithms in Matlab the vector of wave numbers is $[0, \ldots, \frac{N}{2}-1, 0, \frac{-N}{2}+1, \ldots, -1]$.

[7] Here and below, if $x \in [a, b]$, then $\Delta x = \frac{b-a}{N}$, and $x_j = a + j\Delta x, j = 0, 1, \ldots, N$.

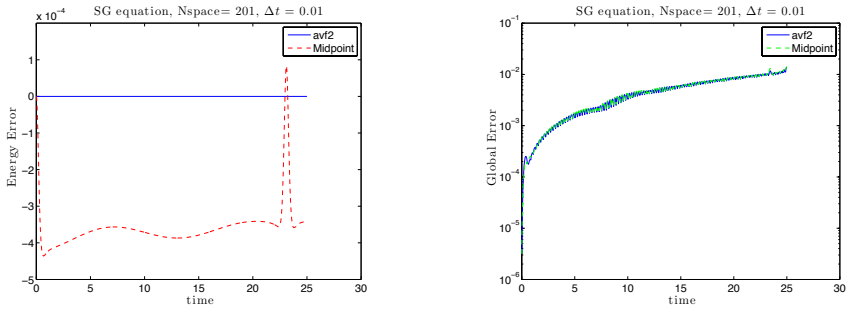

Figure 2.1: Sine-Gordon equation with finite differences semi-discretization: Energy error (left) and global error (right) vs time, for AVF and implicit midpoint integrators.

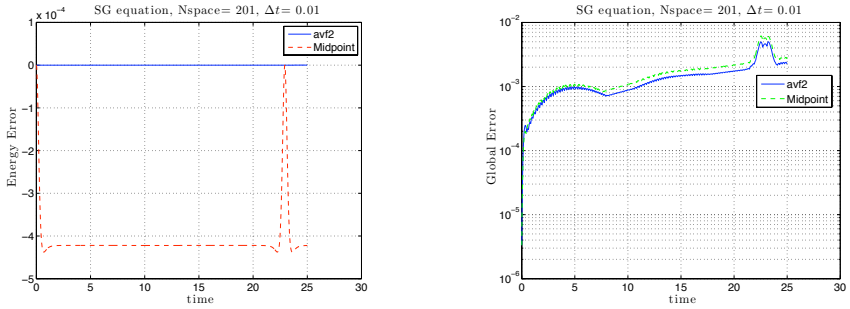

Figure 2.2: Sine-Gordon equation with spectral semi-discretization: Energy error (left) and global error (right) vs time, for AVF and implicit midpoint integrators.

Initial conditions:

$$\left.\begin{aligned} \varphi(x,0) &= 0, \\ \pi(x,0) &= \frac{8}{\cosh(2x)}. \end{aligned}\right\} \quad \text{Right-moving kink and left-moving anti-kink solution.} \tag{2.13}$$

Numerical comparisons of the AVF method with the well known (symplectic) implicit midpoint integrator[8] are given in figure 2.1 for the finite differences discretization, and in figure 2.2 for the spectral discretization.

EXAMPLE 2.2. *Korteweg-de Vries equation:*

Continuous:

$$\frac{\partial u}{\partial t} = -6u\frac{\partial u}{\partial x} - \frac{\partial^3 u}{\partial x^3}, \tag{2.14}$$

[8]Recall that the implicit midpoint integrator is given by $\frac{u_{n+1}-u_n}{\Delta t} = f\left(\frac{u_n+u_{n+1}}{2}\right)$.

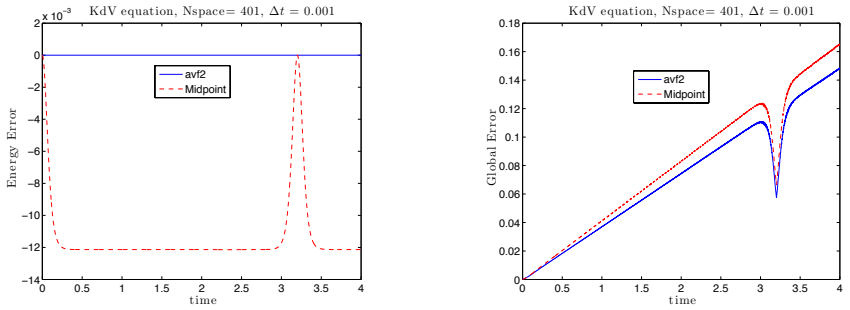

Figure 2.3: Korteweg-de Vries equation: Energy error (left) and global error (right) vs time, for AVF and implicit midpoint integrators.

$$\mathcal{H} = \int \left[\frac{1}{2} (u_x)^2 - u^3 \right] dx, \tag{2.15}$$

$$\mathcal{S} = \frac{\partial}{\partial x}. \tag{2.16}$$

Boundary conditions: periodic, $u(-20, t) = u(20, t)$.

Semi-discrete:

$$\overline{\mathcal{H}} = \sum_j \left[\frac{1}{2(\Delta x)^2} (u_{j+1} - u_j)^2 - u_j^3 \right], \tag{2.17}$$

$$\overline{\mathcal{S}} = \frac{1}{2\Delta x} \begin{bmatrix} 0 & -1 & & & 1 \\ 1 & 0 & -1 & & \\ & \ddots & \ddots & \ddots & \\ & & 1 & 0 & -1 \\ -1 & & & 1 & 0 \end{bmatrix}. \tag{2.18}$$

Initial conditions and numerical data:

$$x \in [-20, 20], \qquad N = 400, \qquad \Delta t = 0.001.$$

Initial condition: $u(x, 0) = 6\ \mathrm{sech}^2(x)$ (for two solitons).

Example 2.3. *Nonlinear Schrödinger equation:*

Continuous:

$$\frac{\partial}{\partial t} \begin{pmatrix} u \\ u^* \end{pmatrix} = \begin{pmatrix} 0 & i \\ -i & 0 \end{pmatrix} \begin{pmatrix} \frac{\delta \mathcal{H}}{\delta u} \\ \frac{\delta \mathcal{H}}{\delta u^*} \end{pmatrix}, \tag{2.19}$$

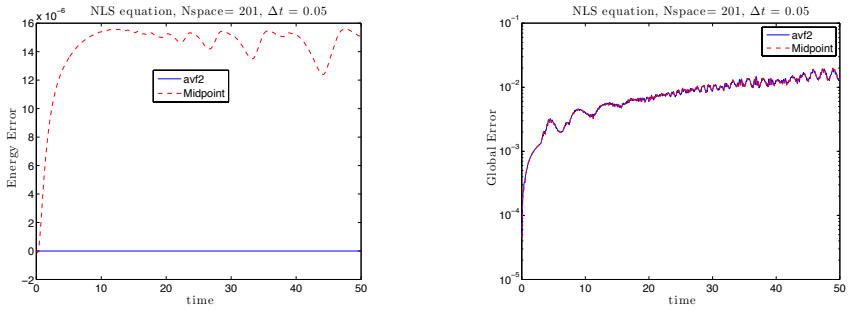

Figure 2.4: Nonlinear Schrödinger equation: Energy error (left) and global error (right) vs time, for AVF and implicit midpoint integrators.

where u^* denotes the complex conjugate of u.

$$\mathcal{H} = \int \left[-\left|\frac{\partial u}{\partial x}\right|^2 + \frac{\gamma}{2}|u|^4 \right] dx, \tag{2.20}$$

$$\mathcal{S} = \begin{pmatrix} 0 & i \\ -i & 0 \end{pmatrix}. \tag{2.21}$$

Boundary conditions: periodic, $u(-20,t) = u(20,t)$.
Semi-discrete:

$$\overline{\mathcal{H}} = \sum_j \left[-\frac{1}{(\Delta x)^2} |u_{j+1} - u_j|^2 + \frac{\gamma}{2}|u_j|^4 \right], \tag{2.22}$$

$$\overline{\mathcal{S}} = i \begin{pmatrix} 0 & \mathrm{id} \\ -\mathrm{id} & 0 \end{pmatrix}. \tag{2.23}$$

Initial conditions and numerical data:

$$x \in [-20, 20], \qquad N = 200, \qquad \Delta t = 0.05, \qquad \text{parameter: } \gamma = 1.$$

Initial conditions:

$$\begin{cases} \Re u(x,0) &= \exp\left(-(x-1)^2/2\right), \\ \Im u(x,0) &= \exp\left(-x^2/2\right). \end{cases} \tag{2.24}$$

EXAMPLE 2.4. *Nonlinear Wave Equation:*
Continuous:

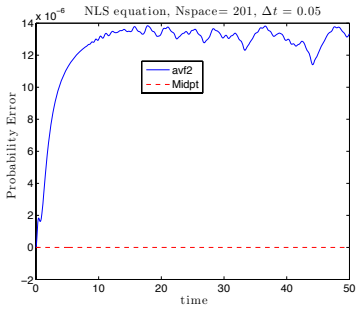

Figure 2.5: Nonlinear Schrödinger equation: Total probability error vs time, for AVF and implicit midpoint integrators.

The 2D wave equation

$$\frac{\partial^2\varphi}{\partial t^2} = \Delta\varphi - \frac{\partial V(\varphi)}{\partial\varphi}, \quad \varphi = \varphi(x,y,t), \quad (x,y) \in [-1,1]\times[-1,1],\, t \geq 0, \tag{2.25}$$

is a Hamiltonian PDE with Hamiltonian function

$$\mathcal{H} = \int_{-1}^{1}\int_{-1}^{1}\left[\frac{1}{2}(\pi^2+\varphi_x^2+\varphi_y^2)+V(\varphi)\right]dx\,dy, \tag{2.26}$$

and the operator $\mathcal{S}$ is the canonical 2×2 symplectic matrix.

Boundary conditions: periodic.

Semi-discrete:

We discretise the Hamiltonian in space with a tensor product Lagrange quadrature formula based on $p+1$ Gauss-Lobatto-Legendre (GLL) quadrature nodes in each space direction. We obtain

(2.27)

$$\overline{\mathcal{H}} = \frac{1}{2}\sum_{j_1=0}^{p}\sum_{j_2=0}^{p} w_{j_1}w_{j_2}\left(\pi_{j_1,j_2}^2+\left(\sum_{k=0}^{p} d_{j_1,k}\varphi_{k,j_2}\right)^2+\left(\sum_{m=0}^{p} d_{j_2,m}\varphi_{j_1,m}\right)^2+\frac{1}{2}\varphi_{j_1,j_2}^4\right),$$

where $d_{j_1,k} = \left.\frac{dl_k(x)}{dx}\right|_{x=x_{j_1}}$, and $l_k(x)$ is the k-th Lagrange basis function based on the GLL quadrature nodes $x_0,\ldots,x_p$, and with $w_0,\ldots,w_p$ the corresponding quadrature weights. The numerical approximation is

$$\varphi_p(x,y,t) = \sum_{k=0}^{p}\sum_{m=0}^{p}\varphi_{k,m}(t)l_k(x)l_m(y), \tag{2.28}$$

and has the property $\varphi_p(x_{j_1},y_{j_2},t) = \varphi_{j_1,j_2}(t)$, so that the data can be stored in the $(p+1)\times(p+1)$ matrix with entries φ_{j_1,j_2}.

Initial conditions and numerical data:

$$(x,y)\in[-1,1]^2, \quad V(\varphi) = \frac{\varphi^4}{4}.$$

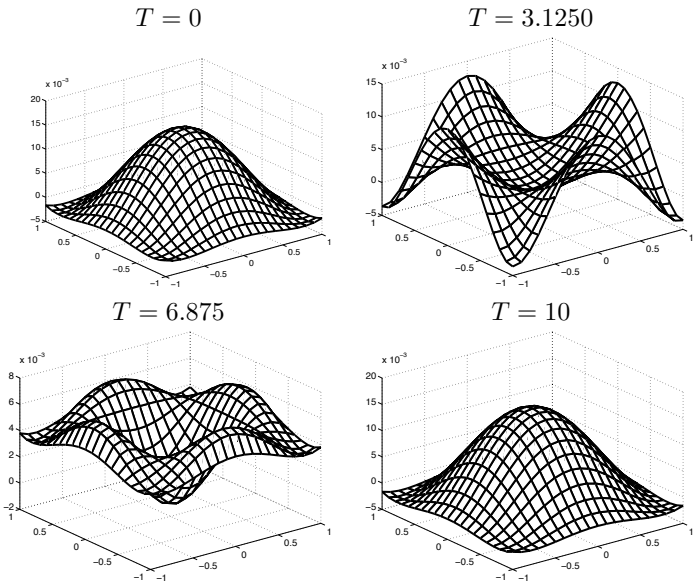

Figure 2.6: Snapshots of the solution of the 2D wave equation at different times. AVF method with step-size $\Delta t = 0.6250$. Space discretization with 6 Gauss Lobatto nodes in each space direction. Numerical solution interpolated on a equidistant grid of 21 nodes in each space direction.

Initial condition: $\varphi(x, y, 0) = \mathrm{sech}(10x)\mathrm{sech}(10y)$, $\pi(x, y, 0) = 0$.

In figure 2.6 we show some snapshots of the solution. The energy error is shown in figure 2.7.

2.2 Linear conservative PDEs

EXAMPLE 2.5. *(Linear) Time-dependent Schrödinger Equation:*
Continuous:

$$\frac{\partial u}{\partial t} = i\frac{\partial^2 u}{\partial x^2} - iV(x)u. \tag{2.29}$$

This equation is bi-Hamiltonian, i.e. it has 2 independent symplectic structures. The first Hamiltonian formulation has

$$\mathcal{H}_1 = \int_{-\pi}^{\pi} \left[-\left|\frac{\partial u}{\partial x}\right|^2 - V(x)\,|u|^2 \right] dx \tag{2.30}$$

and

$$\mathcal{S}_1 = \begin{pmatrix} 0 & i \\ -i & 0 \end{pmatrix}. \tag{2.31}$$

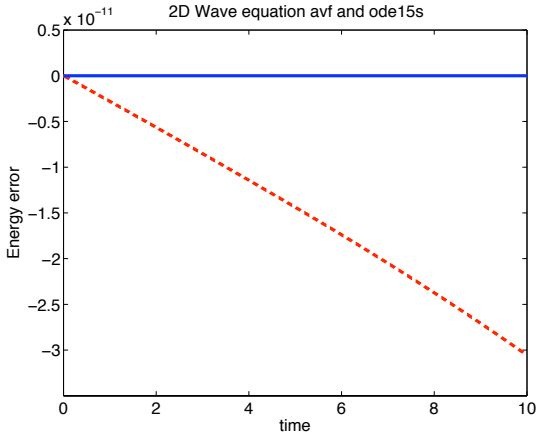

Figure 2.7: The 2D wave equation (2.25). MATLAB routine `ode15s` with absolute and relative tolerance 10^{-14} (dashed line), and AVF method with step size $\Delta t = 10/(2^5)$ (solid line). Energy error versus time. Time interval $[0, 10]$. Space discretization with 6 Gauss Lobatto nodes in each space direction.

The second Hamiltonian formulation has

$$\mathcal{H}_2 = \int_{-\pi}^{\pi} |u|^2 \, dx \tag{2.32}$$

and

$$\mathcal{S}_2 = \begin{pmatrix} 0 & \partial_x^2 - V(x) \\ -\partial_x^2 + V(x) & 0 \end{pmatrix}. \tag{2.33}$$

Boundary conditions: periodic, $u(-\pi, t) = u(\pi, t)$.
Semi-discrete:

$$\overline{\mathcal{H}}_1 = \sum_j \left[-\frac{1}{(\Delta x)^2} |u_{j+1} - u_j|^2 - V(x_j)|u_j|^2 \right], \tag{2.34}$$

$$\overline{\mathcal{S}}_1 = i \begin{pmatrix} 0 & \mathrm{id} \\ -\mathrm{id} & 0 \end{pmatrix}. \tag{2.35}$$

The second semi-discretization is

$$\overline{\mathcal{H}}_2 = \sum_j |u_j|^2, \tag{2.36}$$

$$\overline{\mathcal{S}}_2 = i \begin{pmatrix} 0 & A \\ -A & 0 \end{pmatrix}, \tag{2.37}$$

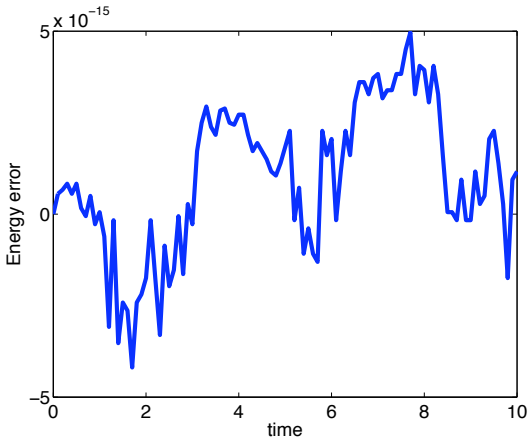

Figure 2.8: Linear Schrödinger equation: Error in energy $\overline{\mathcal{H}}_1 \Delta x$ vs time, AVF method

where

$$A = \begin{pmatrix} -2-V & 1 & 0 & \dots & 1 \\ 1 & -2-V & 1 & & 0 \\ 0 & \ddots & \ddots & \ddots & \vdots \\ 0 & \dots & & & 1 \\ 1 & 0 & \dots & 1 & -2-V \end{pmatrix}. \tag{2.38}$$

Both discretizations result in the same semi-discrete system and the AVF method (which in the linear case coincides with the midpoint rule) therefore preserves both $\overline{\mathcal{H}}_1$ and $\overline{\mathcal{H}}_2$, as well as the two symplectic structures.

Initial conditions and numerical data:

$$x \in [-\pi, \pi], \qquad N = 50, \qquad \Delta t = 0.1, \qquad V(x) = 1 - \cos(x).$$

Initial conditions:

$$\Re u(x,0) = e^{-(\frac{x}{2})^2}, \qquad \Im u(x,0) = 0. \tag{2.39}$$

EXAMPLE 2.6. *Maxwell's Equations (1d):* We first look at the one-dimensional Maxwell equation

Continuous:

$$\frac{\partial}{\partial t} \begin{bmatrix} E \\ B \end{bmatrix} = \begin{bmatrix} 0 & c\frac{\partial}{\partial x} \\ c\frac{\partial}{\partial x} & 0 \end{bmatrix} \begin{bmatrix} \frac{\delta \mathcal{H}}{\delta E} \\ \frac{\delta \mathcal{H}}{\delta B} \end{bmatrix}, \tag{2.40}$$

$$\mathcal{H}(E,B) = \int_0^1 c\frac{1}{2}\left(E^2 + B^2\right) dx, \tag{2.41}$$

and

$$\mathcal{S} = \begin{bmatrix} 0 & \frac{\partial}{\partial x} \\ \frac{\partial}{\partial x} & 0 \end{bmatrix}. \tag{2.42}$$

$\mathcal{S}$ is skew-adjoint on $\{(E,B) \in C^1 : E(0) = E(1) = 0\}$ (and therefore on the Sobolev space H_0^1).

Boundary conditions:

$$\begin{cases} E(0,t) = E(1,t) = 0, \\ \frac{\partial B}{\partial x}(0,t) = \frac{\partial B}{\partial x}(1,t) = 0. \end{cases} \tag{2.43}$$

Semi-discrete:

We now obtain $\overline{\mathcal{H}}$ by discretizing $\mathcal{H}$ in a simple way by applying the trapezoidal rule to the integral (2.41) at the points $x_j = \frac{1}{N}j$ and dividing by Δx, that is

(2.44)
$$\overline{\mathcal{H}}(E_1, \cdots E_{N-1}, B_0, \cdots, B_N) = \sum_{j=1}^{N-1} \left(c\frac{1}{2}E_j^2 \right) + c\frac{1}{4}B_0^2 + \sum_{j=1}^{N-1} \left(c\frac{1}{2}B_j^2 \right) + c\frac{1}{4}B_N^2,$$

where we have already used that $E(x_0,t) = E(x_N,t) = 0$. The differential operator $\mathcal{S}$ is discretized with central differences yielding

$$\overline{\mathcal{S}} = \begin{bmatrix} 0^{N-1,N-1} & G \\ -G^T & 0^{N+1,N+1} \end{bmatrix}, \tag{2.45}$$

where the $(N-1) \times (N+1)$ matrix G is given by

$$G = \frac{1}{2\Delta x} \begin{bmatrix} -2 & 0 & 1 & & & & \\ & -1 & 0 & 1 & & & \\ & & \ddots & \ddots & \ddots & & \\ & & & -1 & 0 & 1 & \\ & & & & -1 & 0 & 2 \end{bmatrix}. \tag{2.46}$$

Initial conditions and numerical data:

Note that the Neumann boundary conditions are satisfied at least to order 1 in space, despite the fact that we only intended to somehow approximate the energy $\mathcal{H}$. The numerical experiments confirm that the discrete energy $\overline{\mathcal{H}}\Delta x$ is preserved to machine precision. Figure 2.9 shows the error of the AVF method for the Maxwell equation with $N = 100$, $\Delta t = 0.001$, $c = 1$, and initial value

$$E(x,0) = e^{-100\left(x-\frac{1}{2}\right)^2}, \qquad B(x,0) = e^{-100\left(x-\frac{1}{2}\right)^2}.$$

EXAMPLE 2.7. *Maxwell's Equations (3D):*

Continuous:

We consider Maxwell's equations in CGS units for the electromagnetic field in a vacuum

$$\frac{\partial}{\partial t} \begin{bmatrix} B \\ E \end{bmatrix} = \begin{bmatrix} 0 & -c\nabla\times \\ c\nabla\times & 0 \end{bmatrix} \begin{bmatrix} B \\ E \end{bmatrix} \tag{2.47}$$

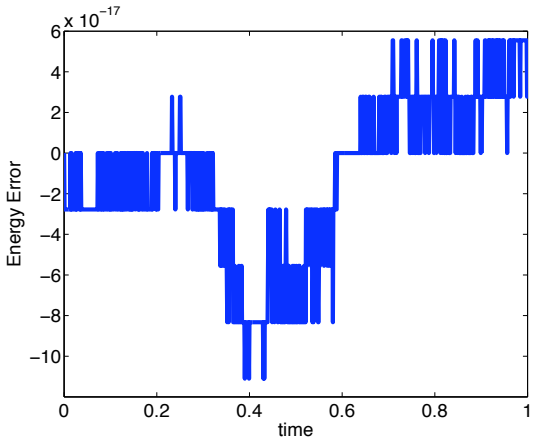

Figure 2.9: One-dimensional Maxwell equation: energy error vs time, AVF integrator.

with the operator

$$\nabla\times := \begin{bmatrix} 0 & -\frac{\partial}{\partial z} & \frac{\partial}{\partial y} \\ \frac{\partial}{\partial z} & 0 & -\frac{\partial}{\partial x} \\ -\frac{\partial}{\partial y} & \frac{\partial}{\partial x} & 0 \end{bmatrix}. \tag{2.48}$$

This equation has two Hamiltonian formulations of type (1.1). The first Hamiltonian formulation has the helicity Hamiltonian

$$\mathcal{H}_1 = \int_Q \left(c\frac{1}{2} B^T (\nabla \times B) + c\frac{1}{2} E^T (\nabla \times E) \right) dxdydz \tag{2.49}$$

(cf. [1]) and the operator

$$\mathcal{S}_1 = \begin{bmatrix} 0 & -I_3 \\ I_3 & 0 \end{bmatrix}, \tag{2.50}$$

where I_3 designates the 3×3 unit matrix. The second Hamiltonian formulation has the Hamiltonian

$$\mathcal{H}_2 = \int_Q \left(c\frac{1}{2} B^T B + c\frac{1}{2} E^T E \right) dxdydz \tag{2.51}$$

(cf. [7]) and the operator

$$\mathcal{S}_2 = \begin{bmatrix} 0 & -\nabla\times \\ \nabla\times & 0 \end{bmatrix}. \tag{2.52}$$

Boundary condition: periodic on the unit cube Q.

Semi-discrete:

On a regular grid with lexicographical ordering in every component of E (resp. B) and concatenating the discretized components gives one discrete vector E_h (resp. B_h), the operator $\nabla\times$ is represented by a matrix A. The discretisation in the first case is given by

$$\overline{\mathcal{H}}_1 = c\frac{1}{2}E_h^T A E_h + c\frac{1}{2}B_h^T A B_h \tag{2.53}$$

and the obvious discretisation of $\mathcal{S}_1$. For the quadratic Hamiltonian,

$$\overline{\mathcal{H}}_2 = c\frac{1}{2}E_h^T E_h + c\frac{1}{2}B_h^T B_h \tag{2.54}$$

and

$$\overline{\mathcal{S}}_2 = \begin{bmatrix} 0 & -A \\ A & 0 \end{bmatrix}. \tag{2.55}$$

Both discretisations result in the same semi-discrete system

$$\begin{bmatrix} \dot{B}_h \\ \dot{E}_h \end{bmatrix} = \begin{bmatrix} 0 & -A \\ A & 0 \end{bmatrix} \begin{bmatrix} B_h \\ E_h \end{bmatrix} \tag{2.56}$$

and the average vector field method preserves both $\overline{\mathcal{H}}_1$ and $\overline{\mathcal{H}}_2$.

Initial conditions and numerical data:

Preservation of $\overline{\mathcal{H}}_1$ and $\overline{\mathcal{H}}_2$ is numerically confirmed by an experiment with random initial data on a regular grid with 30 points in every direction and constant $c = 1$. The result of the AVF method with $\Delta t = 0.01$ can be seen in Figure 2.10.

3 Dissipative PDEs

3.1 Nonlinear dissipative PDEs

EXAMPLE 3.1. *Allen - Cahn equation:*

Continuous:

$$\frac{\partial u}{\partial t} = d u_{xx} + u - u^3, \tag{3.1}$$

$$\mathcal{H} = \int \left[\frac{1}{2} d\,(u_x)^2 - \frac{1}{2}u^2 + \frac{1}{4}u^4\right] dx, \tag{3.2}$$

$$\mathcal{N} = -1. \tag{3.3}$$

Boundary conditions: Neumann, $u_x(0,t) = 0, u_x(1,t) = 0$.

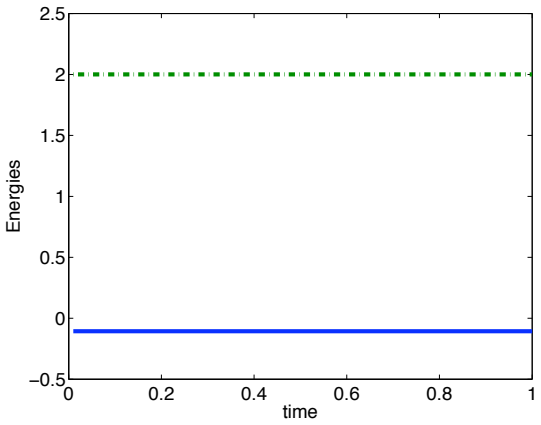

Figure 2.10: Three-dimensional Maxwell equation: plots of energies $\overline{\mathcal{H}}_1\Delta x$ (dash-dot) and $\overline{\mathcal{H}}_2\Delta x$ (dash) vs time.

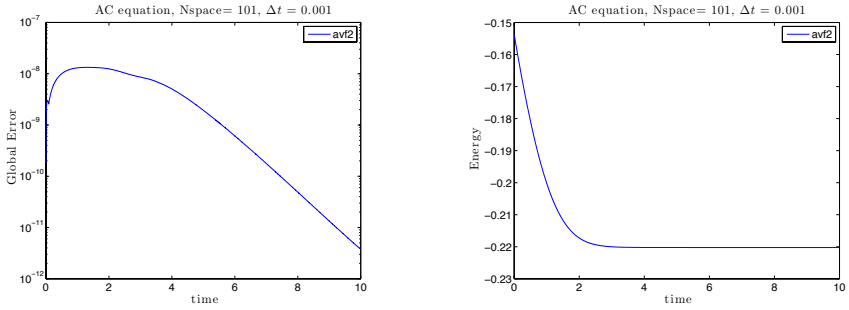

Figure 3.1: Allen-Cahn equation: Global error (left) and energy (right) vs time, AVF integrator.

Semi-discrete:

$$\overline{\mathcal{H}} = \sum_{j=0}^{N} \left[\frac{d}{2(\Delta x)^2} (u_{j+1} - u_j)^2 - \frac{1}{2}u_j^2 + \frac{1}{4}u_j^4 \right], \tag{3.4}$$

$$\overline{\mathcal{N}} = -\mathrm{id}. \tag{3.5}$$

Initial conditions and numerical data:

$$x \in [0,1], \qquad N = 100, \qquad \Delta t = 0.001, \qquad \text{parameter: } d = 0.001.$$

Initial condition: $u(x,0) = \cos(\pi x)$.

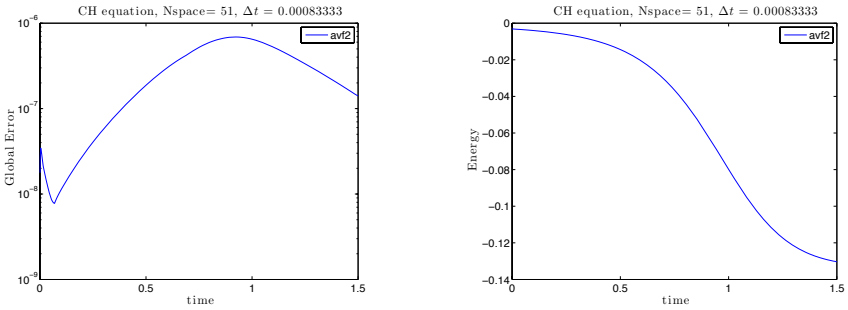

Figure 3.2: Cahn-Hilliard equation: Global error (left) and energy (right) vs time, AVF integrator.

EXAMPLE 3.2. *Cahn-Hilliard equation:*
Continuous:

$$\frac{\partial u}{\partial t} = \frac{\partial^2}{\partial x^2}\left(pu + ru^3 + qu_{xx}\right), \tag{3.6}$$

$$\mathcal{H} = \int \left[\frac{1}{2}pu^2 + \frac{1}{4}ru^4 - \frac{1}{2}q\left(u_x\right)^2\right] dx, \tag{3.7}$$

$$\mathcal{N} = \partial_x^2. \tag{3.8}$$

Boundary condition: periodic, $u(0,t) = u(1,t)$.
Semi-discrete:

$$\overline{\mathcal{H}} = \sum_j \left[\frac{1}{2}pu_j^2 + \frac{1}{4}ru_j^4 - \frac{1}{2}\frac{q}{(\Delta x)^2}\left(u_{j+1} - u_j\right)^2\right], \tag{3.9}$$

$$\overline{\mathcal{N}} = \frac{1}{(\Delta x)^2}\begin{bmatrix} -2 & 1 & & & 1 \\ 1 & -2 & 1 & & \\ & \ddots & \ddots & \ddots & \\ & & 1 & -2 & 1 \\ 1 & & & 1 & -2 \end{bmatrix}. \tag{3.10}$$

Initial conditions and numerical data:

$x \in [0,1], \qquad N = 50, \qquad \Delta t = 1/1200, \quad$ parameters: $p = -1,\ q = -0.001,\ r = 1.$

Initial condition:

$$u(x,0) = 0.1\sin(2\pi x) + 0.01\cos(4\pi x) + 0.06\sin(4\pi x) + 0.02\cos(10\pi x).$$

EXAMPLE 3.3. *Ginzburg-Landau equation:*
Continuous:
A Ginzburg-Landau equation arising in a model of traffic flow is given by

$$\frac{\partial u}{\partial t} = \left(\partial_x - \epsilon\partial_x^2\right)\left[6u + \partial_x^2 u - u^3\right] \tag{3.11}$$

and is a slight modification of the model considered in [14] and [15]. The equation can be written as

$$\frac{\partial u}{\partial t} = \mathcal{N}\frac{\delta \mathcal{H}}{\delta u}, \tag{3.12}$$

with

$$\mathcal{N} = \partial_x - \epsilon\partial_x^2 \tag{3.13}$$

and

$$\mathcal{H} = \int \left[3u^2 - \frac{1}{2}\left(\frac{\partial u}{\partial x}\right)^2 - \frac{1}{4}u^4\right] dx. \tag{3.14}$$

Boundary condition: $u(\pm 5, t) = 0$ and $u_{xx}(\pm 5, t) = 0$.
Semi-discrete:

$$\overline{\mathcal{H}} = \sum_{j=1}^{N-1}\left[3u_j^2 - \frac{1}{2}\left(\frac{u_{j+1} - u_j}{\Delta x}\right)^2 - \frac{1}{4}u_j^4\right], \qquad u_N = 0. \tag{3.15}$$

and

$$\overline{\mathcal{N}} = A - \epsilon B, \tag{3.16}$$

where

$$A = \frac{1}{2\Delta x}\begin{bmatrix} 0 & 1 & & & \\ -1 & 0 & 1 & & \\ & \ddots & \ddots & \ddots & \\ & & -1 & 0 & 1 \\ & & & -1 & 0 \end{bmatrix} \tag{3.17}$$

is a discretisation of ∂_x, and

$$B = \frac{1}{(\Delta x)^2}\begin{bmatrix} -2 & 1 & & & \\ 1 & -2 & 1 & & \\ & \ddots & \ddots & \ddots & \\ & & 1 & -2 & 1 \\ & & & 1 & -2 \end{bmatrix} \tag{3.18}$$

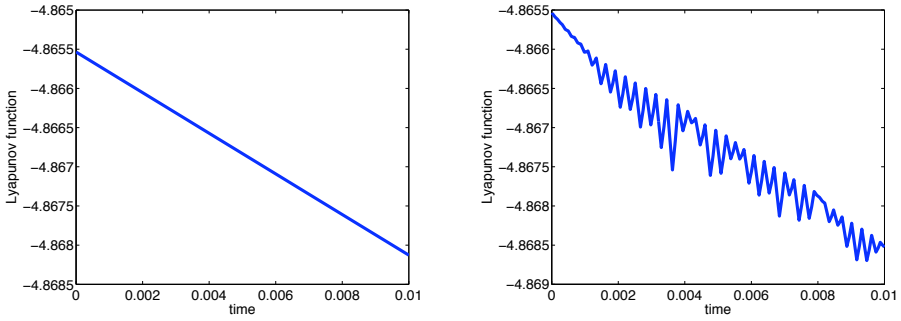

Figure 3.3: Ginzburg-Landau equation: Plots of the energy function $\overline{\mathcal{H}}\Delta x$ computed with the AVF method (left) and Matlab's `ode45` (right). Note that `ode45` does not exhibit the correct monotonic decrease in energy.

is a discretisation of ∂_x^2. The average vector field method preserves the decay of function $\overline{\mathcal{H}}$ in contrast to some standard integrators.

Initial conditions and numerical data:

$$x \in [-5, 5], \qquad N = 100, \qquad \Delta t = 0.001, \quad \text{parameter: } \epsilon = -10^{-6}.$$

Initial condition: $u(x,0) = e^{-100\left(x-\frac{1}{2}\right)^2}$.

In Figure 3.3, we compare the AVF method with Matlab's `ode45`, the latter not preserving the monotonic decay of $\overline{\mathcal{H}}$.

3.2 Linear dissipative PDEs

EXAMPLE 3.4. *Heat equation:*

Continuous:

The heat equation

$$\frac{\partial u}{\partial t} = u_{xx}, \tag{3.19}$$

is a dissipative PDE and can be written in the form (1.1), i.e.

$$\frac{\partial u}{\partial t} = \mathcal{N}_1 \frac{\delta \mathcal{H}_1}{\delta u}, \qquad \frac{\partial u}{\partial t} = \mathcal{N}_2 \frac{\delta \mathcal{H}_2}{\delta u}, \tag{3.20}$$

with the Lyapunov functions $\mathcal{H}_1(u) = \int_0^1 \frac{1}{2} u_x^2 \, dx$ and $\mathcal{H}_2(u) = \int_0^1 \frac{1}{2} u^2 \, dx$ and the operators $\mathcal{N}_1 = -1$ and $\mathcal{N}_2 = \partial_x^2$, respectively.

Boundary conditions: $u(0,t) = u(1,t) = 0$.

Semi-discrete:

$$\overline{\mathcal{H}}_1 = \frac{1}{2(\Delta x)^2} \left[u_1^2 + \sum_{j=2}^{N-1} (u_j - u_{j-1})^2 + u_{N-1}^2 \right] \tag{3.21}$$

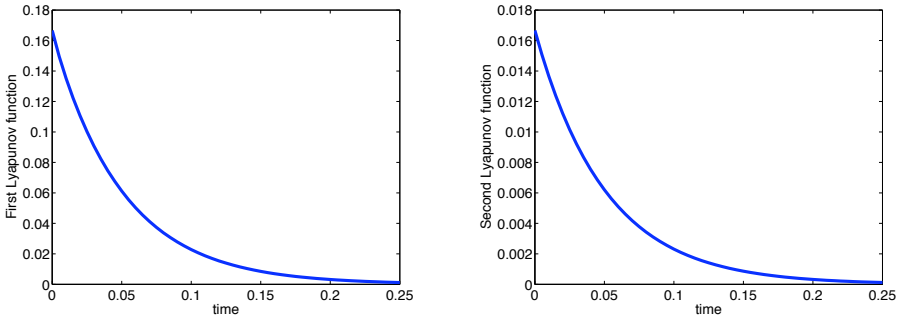

Figure 3.4: Heat equation: plots of Lyapunov functions $\overline{\mathcal{H}}_1\Delta x$ (left) and $\overline{\mathcal{H}}_2\Delta x$ (right) vs time, AVF integrator.

and

$$\overline{\mathcal{H}}_2 = \sum_{j=1}^{N-1} \frac{1}{2}(u_j)^2, \tag{3.22}$$

as well as

$$\overline{\mathcal{N}}_2 = \frac{1}{(\Delta x)^2}\begin{bmatrix} -2 & 1 & & & \\ 1 & -2 & 1 & & \\ & \ddots & \ddots & \ddots & \\ & & 1 & -2 & 1 \\ & & & 1 & -2 \end{bmatrix} \tag{3.23}$$

and the obvious discretisation of $\mathcal{N}_1$. With these choices, both discretisations yield identical semi-discrete equations of motion and therefore $\overline{\mathcal{H}}_1$ and $\overline{\mathcal{H}}_2$ are simultaneously Lyapunov functions of the semi-discrete system and therefore, the AVF integrator preserves both Lyapunov functions.

Initial conditions and numerical data:

$$x \in [0,1], \qquad N = 50, \qquad \Delta t = 0.0025. \tag{3.24}$$

Initial condition: $u(x,0) = x(1-x)$.

This system is numerically illustrated in Figure 3.4, where the monotonic decrease of the Lyapunov functions for the heat equation in (3.21) and (3.22) is shown.

4 Concluding Remarks

The concept of energy, i.e. its preservation or dissipation, has far reaching consequences in the physical sciences. Therefore many methods to preserve energy, and several to preserve the correct dissipation of energy (e.g. [6, 11]), have

been proposed for ordinary differential equations. Surprisingly, when partial differential equations are considered, a unified way to discuss the preservation or correct dissipation of energy is missing and similar ideas are often developed from scratch (e.g. [5, 10]). In this paper, we have presented a systematic and unified way to discretise partial differential equations and to preserve their correct energy preservation, or dissipation, by the average vector-field method.

For the equations treated in this paper, one can replace the average vector-field method by any energy-preserving B-series method, while retaining the advantageous properties of energy preservation or dissipation. More generally, geometric integrators for Hamiltonian or non-Hamiltonian PDEs with non-constant matrix $\mathcal{D}$ can be constructed using discrete gradient methods, cf. [11].

Acknowledgements.

This research is supported by the Australian Research Council. We are grateful to Will Wright for many useful discussions.

REFERENCES

1. N. Anderson and A.M. Arthurs, *Helicity and variational principles for Maxwell's equations*, Int. J. Electronics, 54 (1983), pp. 861–864.
2. W.L. Briggs and V.E. Henson, *The DFT: An Owner's Manual for the Discrete Fourier Transform*, SIAM, 1995.
3. E. Celledoni, R.I. McLachlan, D.I. McLaren, B. Owren, G.R.W. Quispel, and W.M. Wright, *Energy-preserving Runge-Kutta methods*, Preprint, submitted, 2008.
4. R.P. Feynman. *Conservation of energy. Chapter 4, Volume 1, The Feynman Lectures on Physics*, Addison-Wesley Pub. Co., 1965.
5. D. Furihata, *Finite Difference Schemes for* $\frac{\partial u}{\partial t} = \left(\frac{\partial}{\partial x}\right)^{\alpha} \frac{\delta G}{\delta u}$ *that Inherit Energy Conservation or Dissipation Property*, J. Comput. Phys., 156 (1999), pp. 181–205.
6. V. Grimm and G.R.W. Quispel *Geometric integration methods that preserve Lyapunov functions*, BIT, 45 (2005), pp. 709–723.
7. T. Hirono, W. Lui, S. Seki and Y. Yoshikuni, *A three-dimensional fourth-order Finite-Difference Time-Domain scheme using a symplectic integrator propagator*, IEEE Trans. Microwave Theory and Tech., 49 (2001), pp. 1640–1648.
8. A. Iserles, *A First Course in the Numerical Analysis of Differential Equations*, Cambridge University Press, 1996.
9. S. Klainerman, *Partial differential equations* in The Princeton Companion to Mathematics, T. Gowers, Ed. Princeton University Press, 2008, pp.455–483.
10. T. Matsuo. *New conservative schemes with discrete variational derivatives for nonlinear wave equations*, J. Comput. Appl. Math., 203 (2007), pp. 32–56.
11. R.I. McLachlan, G.R.W. Quispel, and N. Robidoux. *Geometric integration using discrete gradients*, Phil. Trans. Roy. Soc. A, 357 (1999), pp. 1021–1045.
12. R.I. McLachlan and N. Robidoux. *Antisymmetry, pseudospectral methods, weighted residual discretizations, and energy conserving partial differential equations*, Preprint, 2000.
13. R.I. McLachlan and N. Robidoux. *Antisymmetry, pseudospectral methods, and conservative PDEs*, in International Conference on Differential Equations, Vol. 1, 2 (Berlin, 1999), World Sci. Publ., River Edge, NJ, 2000, pp. 994–999. .

14. Eq(27) in: T. Nagatani. *Thermodynamic theory for the jamming transition in traffic flow*, Phys. Rev. E, 58 (1998), pp. 4271–4276.
15. T. Nagatani. *Time-dependent Ginzburg–Landau equation for the jamming transition in traffic flow*, Physica A, 258 (1998), pp. 237–242.
16. P. Olver, *Applications of Lie Groups to Differential Equations, Second Edition*, Springer-Verlag, New York, 1993.
17. G.R.W. Quispel and D.I. McLaren. *A new class of energy-preserving numerical integration methods*, J. Phys. A: Math. Theor., 41 (2008), 045206 (7pp).
18. L.N. Trefethen, *Spectral Methods in MATLAB*, SIAM, 2000.

5 APPENDIX

PROOF OF LEMMA 1.1
We denote the consistent discretisation of

$$\mathcal{H}[u] = \int_\Omega H(x; u^{(n)})\, dx \tag{5.1}$$

by

$$\overline{\mathcal{H}}'[u] = \sum_{\overline{\Omega}} a_n \overline{H}(x_n; \overline{u}_{(n+k)})\Delta x. \tag{5.2}$$

Here $\overline{\mathcal{H}}' = \overline{\mathcal{H}}\Delta x$, and $\overline{u}_{(n+k)}$ denotes the set

$$\begin{aligned}\big\{\overline{u}_1(n+k_{1,1}),\dots,\ \overline{u}_1(n+k_{1,p}); \overline{u}_2(n+k_{2,1}),\dots,\overline{u}_2(n+k_{2,p});\\ \dots;\ \overline{u}_m(n+k_{m,1}),\dots,\overline{u}_m(n+k_{m,p})\big\},\end{aligned} \tag{5.3}$$

where n and the $k_{i,j}$ are discrete vectors in $\mathbb{Z}^d$, and $\overline{\Omega}$ is some discrete approximation to Ω.

The discrete analogue of the variational derivative $\dfrac{\delta\mathcal{H}}{\delta u}$ is then defined by

$$\begin{aligned}\frac{d}{d\varepsilon}\overline{\mathcal{H}}'(\overline{u}+\varepsilon\overline{v})\big|_{\varepsilon=0} &=: \sum_{\overline{\Omega}} \left(\frac{\delta\overline{\mathcal{H}}'}{\delta\overline{u}}\right)_n \cdot \overline{v}_n\ \Delta x\\ &= \left(\overline{v}\cdot\frac{\delta\overline{\mathcal{H}}'}{\delta\overline{u}}\right)\Delta x.\end{aligned} \tag{5.4}$$

We now calculate the l.h.s. of eq.(5.4):

$$
\begin{aligned}
(5.5)\qquad & \frac{d}{d\varepsilon}\overline{\mathcal{H}}'(\overline{u}+\varepsilon\overline{v})\big|_{\varepsilon=0} \\
&= \frac{d}{d\varepsilon}\sum_{\overline{\Omega}} a_n \overline{H}(x_n; \overline{u}_1(n+k_{1,1})+\varepsilon\overline{v}_1(n+k_{1,1}), \\
&\quad \ldots, \overline{u}_m(n+k_{m,p})+\varepsilon\overline{v}_m(n+k_{m,p}))\big|_{\varepsilon=0} \\
&= \sum_{\overline{\Omega}} \big[a_{n-k_{1,1}}\overline{H}_2(x_{n-k_{1,1}}; \overline{u}_1(n), \ldots, \overline{u}_m(n+k_{m,p}-k_{1,1}))\ldots \\
&\quad + a_{n-k_{m,p}}\overline{H}_{mp+1}(x_{n-k_{m,p}}; \overline{u}_1(n+k_{1,1}-k_{m,p}), \ldots, \overline{u}_m(n))\big]\cdot \overline{v}_n\Delta x \\
&= \sum_{\overline{\Omega}} \big[\frac{\partial}{\partial u_n}\sum_{q,r} S_{-k_{q,r}}\overline{H}(x_n, \overline{u}_1(n+k_{1,1}), \ldots, \overline{u}_m(n+k_{m,p}))\big]\cdot \overline{v}_n\Delta x
\end{aligned}
$$

where S_a denotes the shift over the multi-index a.

It follows that

$$
\frac{d}{d\varepsilon}\overline{\mathcal{H}}'(\overline{u}+\varepsilon\overline{v})\big|_{\varepsilon=0} = (\overline{v}\cdot\nabla\overline{\mathcal{H}}'). \tag{5.6}
$$

Since eqs (5.4) and (5.6) must hold for all vectors $\overline{v}$, we have

$$
\frac{\delta\overline{\mathcal{H}}'}{\delta\overline{u}}\Delta x \equiv \nabla\overline{\mathcal{H}}', \tag{5.7}
$$

and hence

$$
\frac{\delta\overline{\mathcal{H}}'}{\delta\overline{u}} \equiv \nabla\overline{\mathcal{H}}. \tag{5.8}
$$

□

While the proof above is for a scalar function u, the case where u is vector-valued follows in a similar fashion.